

Supplementary Information

Treatment of Cystic Fibrosis Airway Cells with CFTR Modulators Reverses Aberrant Mucus Properties via Hydration

Cameron B. Morrison¹, Kendall M. Shaffer¹, Kenza C. Araba¹, Matthew R. Markovetz¹, Jason A. Wykoff¹, Nancy L. Quinney¹, Shuyu Hao⁵, Martial F. Delion¹, Alexis L. Flen¹, Lisa C. Morton¹, Jimmy Liao¹, David B. Hill^{1,3}, Mitchell L. Drumm⁴, Wanda K. O'Neal¹, Mehmet Kesimer¹, Martina Gentsch^{1,2,5} and *Camille Ehre^{1,2}

Supplementary Methods

Calu3 cell mutagenesis: The CFTR-KO Calu3 cell line was generated by CRSIPR/Cas9-mediated mutagenesis, in which a guide RNA (gRNA) recognizing CFTR exon 11 was used to introduce a premature stop codon [1]. Similar manipulations were performed with the WT line using a gRNA matching the endogenous genome sequence and therefore no detectable mutation was identified in CFTR. In the CFTR-KO line, all alleles of CFTR carried a frameshift insertion, c.1433.insG. Note, PCR primers bind to a sequence in exon 10, which is located in 5' of the mutagenesis site. The CFTR mutagenesis was confirmed by CFTR protein and function, assessed by western blot and short circuit currents, respectively [1].

Calu3 cell culture: Calu3 cells (WT and CFTR-KO lines) were grown at air-liquid interface on 12mm Transwells or Snapwells (Corning, Corning NY) seeded at a density of 2×10^5 cells/cm² and maintained at 5% CO₂ and 37°C. Cells were fed basolaterally with MEM α media (Gibco, Gaithersburg, MD) plus 10% FBS (VWR, Radnor, PA) and 1% penicillin/streptomycin (Sigma-Aldrich, St. Louis, MO) every two days. Once confluent, cells were allowed to differentiate and accumulate mucus for 10-14 days before experimentation. To determine the integrity of Calu3 cell monolayers grown on inserts, transepithelial resistance (Rt) was measured using an EVOM device and revealed an average TEER value of 420 Ω *cm².

Histology and Immunohistochemistry: Calu3 cell cultures fixed in 4% PFA and embedded in paraffin were prepared as histological sections. After deparaffinization, sections were stained with hematoxylin and eosin (H&E), alcian-blue periodic acid Schiff (AB-PAS), or processed for immunohistochemistry (IHC), as described in Ehre et al. [2]. Briefly, IHC unstained sections underwent epitope retrieval using heated 1X citrate buffer in Deionized water and were blocked for 1h in 3% Bovine Serum Albumin (BSA) solution. Primary antibodies: mouse anti-MUC5AC 45M1 (Invitrogen MA5-12178) and rabbit anti-MUC5B (UNC414 from Ehre lab) were co-applied

overnight at 4°C, followed by secondary antibodies (anti-mouse Alexa Fluor 594 and anti-rabbit Alexa Fluor 488) incubation for 1h at room temperature. Slides were incubated with DAPI (Invitrogen 2031179) for 5 min at room temperature and mounted using FluorSave Reagent (Millipore Sigma 345789). Fluorescence was detected with a VS120 virtual scanning microscope (Olympus Microscopy, Shinjuku, Japan).

Primary HBE cell cultures: Primary human bronchial epithelial (HBE) cells were harvested from normal post-mortem and CF lungs at the time of transplantation and were selected according to specific mutations responding to modulator therapies (i.e., heterozygote G551D responding to VX-770 and homozygote F508del responding to ETI) as previously described [3, 4]. The protocol for lung dissection and cell collection was approved by University of North Carolina Institutional Review Board. In brief, cells were grown at ALI on 12 mm Transwells or Snapwells inserts coated with 7.5µg/cm² type IV collagen (Sigma C-7521) with PneumaCult-Ex Plus media (StemCell Technologies, Vancouver, Canada) for 3-5 days. Once confluent, cells were switched to air-liquid interface and differentiated with PneumaCult-ALI media basolaterally for four weeks. Cells were allowed to accumulate mucus for two weeks before experimentation.

Modulator treatment *in vitro*: Once differentiated, tissue cultures were treated for 3-5 days with vehicle (DMSO) or CFTR modulator compounds. For G551D cultures, 0.05% DMSO or 5µM VX-770 was applied to the basolateral media every 24h. For F508del cultures, 0.06% DMSO or 1µM VX-770, 2µM VX-445, and 3µM VX-661 (ETI) was applied to the basolateral media every 24h. Following treatment, cells were washed apically with regular PBS, PBS alkalized by 0.3 pH unit with NaOH or HCO₃⁻ or 1mM tris (2-carboxyethyl) phosphine (TCEP) for 15 minutes. Samples washed with TCEP were quenched with equimolar iodoacetamide after collection to stop the reduction reaction. For long washes, cells were washed with PBS for 3 hours.

Bioelectrical measurements: Electrophysiological properties were measured by Ussing chamber as described by Fulcher et al [5]. In brief, cell inserts were mounted on Ussing chambers

(Physiologic Instruments, San Diego, CA) and short-circuit currents (I_{sc}) were measured under basal condition and following the addition of 10 μ M forskolin (mucosal and serosal) to activate CFTR, 5 μ M VX-770 (mucosal and serosal), 10 μ M CFTR inhibitor 172 (CFTR_{inh}-172) (mucosal) to inhibit CFTR-specific current. Data were collected and analyzed using Acquire and Analysis software (Physiologic Instruments).

Gene expression by qPCR: For mRNA expression, cells were lysed in Trizol and processed for total mRNA extraction, cDNA reverse transcription, and quantitative PCR as described by Chen et al [6]. In brief, total RNA was purified via the direct-Zol RNA miniprep kit (Zymo Research, Irvine, CA). RNA was reverse transcribed to cDNA and qPCR was performed using Taqman probes for GAPDH, CFTR, MUC5AC, and MUC5B (Applied Biosystems, Foster City, CA) and the QuantStudio6 real-time PCR machine (Applied Biosystems). The house-keeping gene used for normalization was GAPDH.

Measurement of pH: To maintain cell viability, Krebs-Ringer buffer (150 μ L) was applied apically to each insert and allowed to equilibrate for 4hrs at 37°C and 5% CO₂ in a temperature- and CO₂-controlled chamber (Controlled Atmosphere In Vitro Glove Box, Coy Laboratory Products Inc., Grass Lake, MI). Note, to mimic *in vivo* conditions, cells were not washed prior to pH measurement and mucus was allowed to remain on the cell surfaces. Once equilibration was reached (Figure S2A), apical pH was measured inside the sealed chamber using a microprobe (In-Lab Ultra-Micro-ISM, Mettler Toledo, Columbus, OH). Two measurements were taken per insert and averaged for each data point with controls (empty wells without cells) measured in parallel for quality control.

SEC-MALS: To measure total mucin concentration, size-exclusion chromatography multi-angled light scattering was used as described by Henderson et al [7]. In brief, 30 min cell washes were diluted 1:1 with 6M GuHCl immediately upon collection. An aliquot (100 μ l) of the diluted cell washes was chromatographed on a Sepharose CL-2B size exclusion column (15 \times 2.5 cm) and

eluted with 0.2M NaCl (with 10 mM EDTA) at a flow rate of 500 μ l/minute. The column effluent was passed through an in-line enhanced optical system laser photometer (Dawn; Wyatt Technology) coupled to a digital signal-processing interferometric refractometer (Optilab; Wyatt Technology) to continuously measure light scattering and sample concentrations, respectively. Data were integrated and analyzed with the Astra software provided with the Dawn laser photometer and absolute values of mucin concentration were determined from the differential refractometry by measuring the specific refractive index increment (dn/dc) that reflects the deviation of the refractive index by concentration. A dn/dc of 0.165 ml/g was used for mucins.

Mucin western blot: Relative abundance of MUC5AC and MUC5B was analyzed by mucin western blotting as previously described by Ramsey et al [8]. Samples were collected via 15 min washes with PBS or 1mM TCEP. Reduced samples were quenched with 1mM iodoacetamide to stop reduction. Cell washing samples (40 μ l) were separated by electrophoresis using an 0.8% agarose gel (80V) for 60 min. Samples were then vacuum transferred to a 0.45 μ m nitrocellulose membrane. Following transfer, membranes were blocked for 1h at RT and probed with 45M1 mouse-anti-MUC5AC (Invitrogen MA5-12178, Invitrogen, Carlsbad, CA) and H-300 rabbit-anti-MUC5B (Santa Cruz SC-20119, Santa Cruz Biotechnology, Dallas, TX) overnight at 4°C. Membranes were rinsed in PBS and then probed for secondary detection with 1 μ g/mL donkey-anti-mouse (Li-Cor 926-68022, Li-Cor, Lincoln, NE) and donkey-anti-rabbit (Li-Cor 926-32213) for 1h at RT. Relative mucin abundance was quantified using Li-Cor Odyssey software.

Scanning electron microscopy: To maintain the mucin network ultrastructure, unwashed cultures were gently submerged in 2.5% glutaraldehyde in 0.1M sodium cacodylate buffer (Electron Microscopy Sciences, Hatfield, PA) overnight at 4°C. Samples were washed with fixative-free buffer 3x before dehydration in increasing concentrations of ethanol (30-100%). Samples were then dried by bringing them through the critical point in liquid CO₂ (Tousimis, Rockville, Maryland) and sputter coated with 8nm of gold-palladium alloy (Ted Pella, Redding,

CA). Images were acquired on a Zeiss Supra 25 field emission SEM (Zeiss, Oberkochen, Germany) at 5kV and a working distance of 5mm. Imaging was performed at the UNC Microscopy Services Laboratory. Photoshop software was used for image colorization (Figure S4).

For pore size measurements, we used the ImageJ software to select the larger pores by inducing contrast and measuring the diameter (e.g., averaging of 3 measurements per pore), 15 pores per image, and 3 images per group.

Microbead rheology: To assess the biophysical properties of mucus, we performed particle-tracking microrheology (PTM) on short (15 min) and long (1h) PBS cell washings, as previously described by Markovetz et al [9]. In brief, the thermally driven motion of 1 μm diameter carboxylated fluorescent beads (Fluospheres, Thermo Fisher, Fremont, CA) was tracked to determine the viscoelastic properties of the gel. Bead motion was recorded for 30 seconds at a rate of 60 frames/sec using a 40x air objective on a Nikon Eclipse TE2000U microscope. Individual bead trajectories were measured automatically using a custom Python program that uses TrackPy (doi: 10.5281/zenodo.34028) for bead localization and tracking. Bead motion was converted into mean squared displacements (MSD) and complex viscosity (η^*) values. For each group, 6 inserts were washed, 3 wash aliquots (5 μL each) were imaged per insert, 8 videos were captured per aliquot and roughly 5 to 30 beads were tracked per video.

Ciliary beat frequency (CBF) Cilia beat frequency (CBF) was determined by taking phase contrast videos of the field of view and performing Fourier spectral analysis on each pixel as a function of time. Twenty-second videos were recorded at 60 frames/sec using a FLIR Grasshopper 3 camera and a 40x objective. Videos were imported into MATLAB, where each pixel was stored as an array of grayscale values versus time. Each array was windowed and then transformed via fast Fourier transform. The dominant peak in the power spectrum was selected and checked against the next highest peaks (2.5 standard deviations away in power) to determine each pixel's light intensity fluctuation frequency and to make sure that the signal was distinct from

the noise. Frequencies were reported for each pixel, and the average of all the pixels with nonzero frequencies was used to determine the CBF for a field of view [10].

Percent solid measurements: The percentage of mucus solid content, an index of hydration, was calculated by measuring dry-to-wet weight ratio of 25 μ l of mucus directly pipetted from the cell surfaces (24 mm Transwell inserts) with a positive displacement pipet (Microman, Gilson), as previously described in [7]. Measurements were performed using a calibrated microbalance (XSR105 DualRange, Mettler Toledo) on mucus collected from non-treated and ETI-treated F508del cells. Airway mucus is comprised of 1% salt electrolytes [11]; hence salt components can be subtracted from the total % solids to obtain % organic content.

Mucociliary transport velocity measurements: Fluorescent carboxylated beads can bind to the cilia when nebulized directly onto the cells. Hence, for *in situ* mucus transport measurements, we used red blood cells (RBC) since their surface chemistry is designed to not interfere with mucus transport. To prevent coagulation and cell lysis, RBC collected from laboratory samples were hardened by exposure to 0.08% glutaraldehyde, centrifuged 500xg for 10 min and resuspended in PBS. To measure mucus velocity rates, 2 μ l of hardened RBC solution were added apically to the center of the cell cultures. RBC were allowed to disperse for 15 min before imaging. Following RBC dispersion, four specific regions (center and three edges) of the inserts were imaged for 30 sec with a dissecting microscope (SPZV-50E, AVEN Inc.) at 1.5X magnification and 60 frames/s (see videos). On average, 12 RBC streaks (spreading from center to edge) were tracked per insert and the distance travelled was calculated using ImageJ (ImageJ, National Institutes of Health, Bethesda, Maryland, USA). Mucus velocity rate was determined in μ m/sec for 4 inserts before and after a 3-day ETI treatment. Mucus transport measurements were done at day 3 of treatment but active transport became apparent as early as 12hr after treatment onset.

Statistical analysis: Statistical analysis was performed using GraphPad Prism (GraphPad Software, San Diego, CA). Comparisons between two groups were performed using Student's two-tailed unpaired t-tests. Significance was assessed at $P < 0.05$. Error bars are shown as SEM.

Supplementary Figure

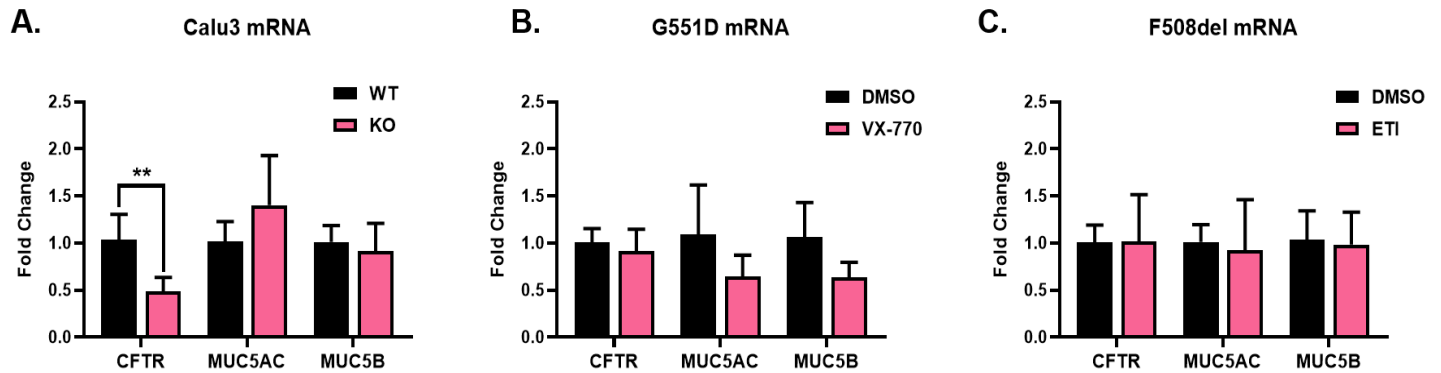


Figure S1. Quantitative PCR analysis of Calu3, G551D and F508del cells for CFTR, MUC5B and MUC5AC gene expression. Expression for CFTR, MUC5B, and MUC5AC genes was measured via qRT-PCR and normalized to WT values. **A.)** CFTR, MUC5B, and MUC5AC mRNA expression in WT and CFTR-KO Calu3 cells, n=6, ** $P < 0.01$. **B.)** CFTR, MUC5B, and MUC5AC mRNA expression in primary G551D HBE cells treated with vehicle (DMSO) or VX-770, n=5. **C.)** CFTR, MUC5B, and MUC5AC mRNA expression in primary F508del cells treated with vehicle or ETI, n=5-6.

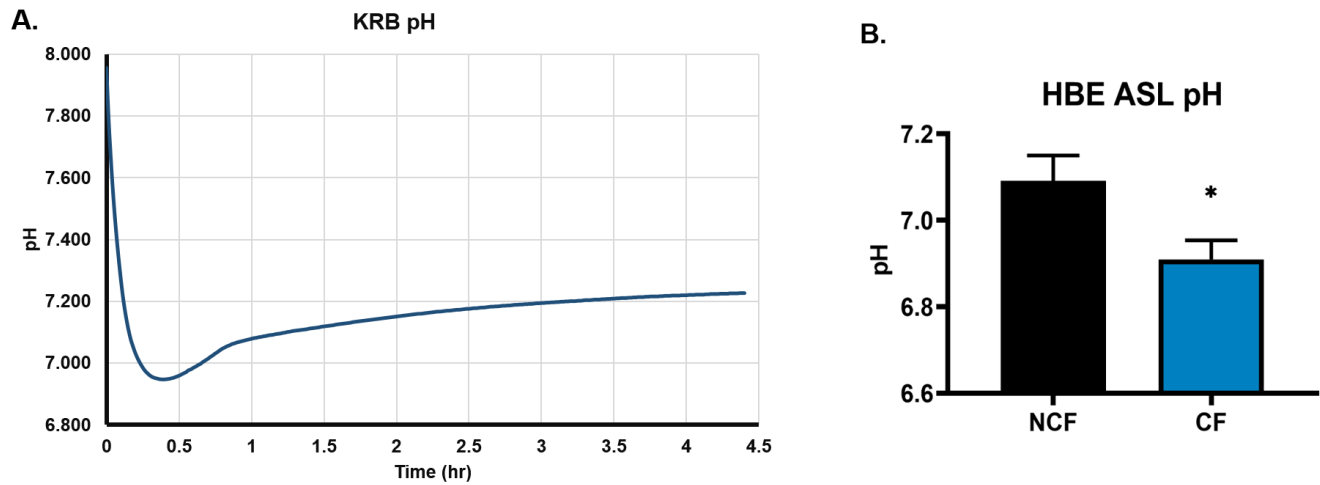


Figure S2. Validation of *in vitro* ASL pH measurements. Krebs Ringers buffer was used to measure apical pH with a microprobe in a CO₂ and temperature-controlled chamber. **A.)** KRB pH as a function time as the buffer equilibrates to 37°C and 5% CO₂ from ambient conditions. **B.)** ASL pH measurements from non-CF (NCF) and CF HBE cells to confirm this technique can measure differences in ASL pH consistent with *in vivo* reports, n=3 donors for non-CF and n=5 donors for CF lungs. For each donor, an average of 6-8 inserts was measured. * $P < 0.05$.

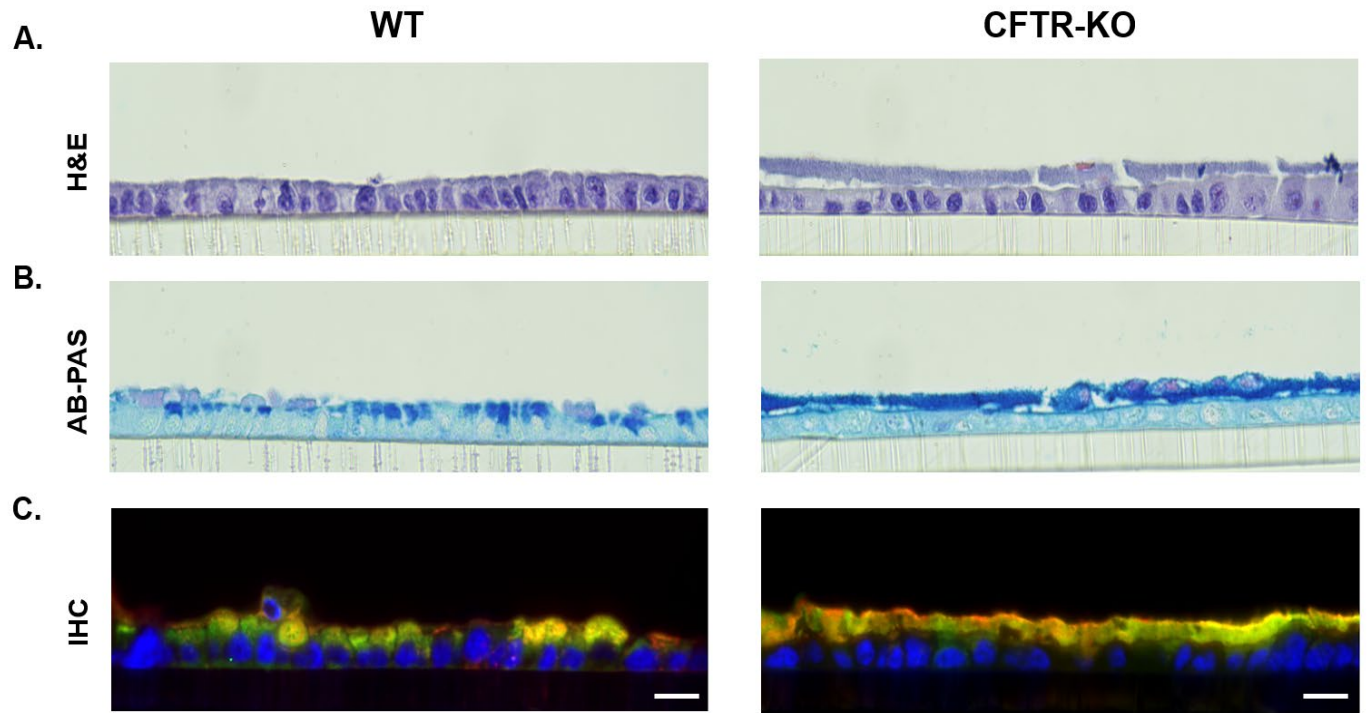


Figure S3. Histological appearance and mucin labeling of WT and CFTR- KO Calu3 cell cultures. A.) Representative images of WT and CFTR-KO Calu3 cell cultures stained with hematoxylin and eosin (H&E) to examine the cellular organization of the two cell lines. **B.)** Representative images of histological sections stained with alcian-blue periodic acid Schiff (AB-PAS) to detect the oligosaccharides decorating airway mucins. **C.)** Immunohistochemistry (IHC) individually labeling MUC5AC (red), MUC5B (green), and DAPI (blue). Scale bar is 20 μ m.

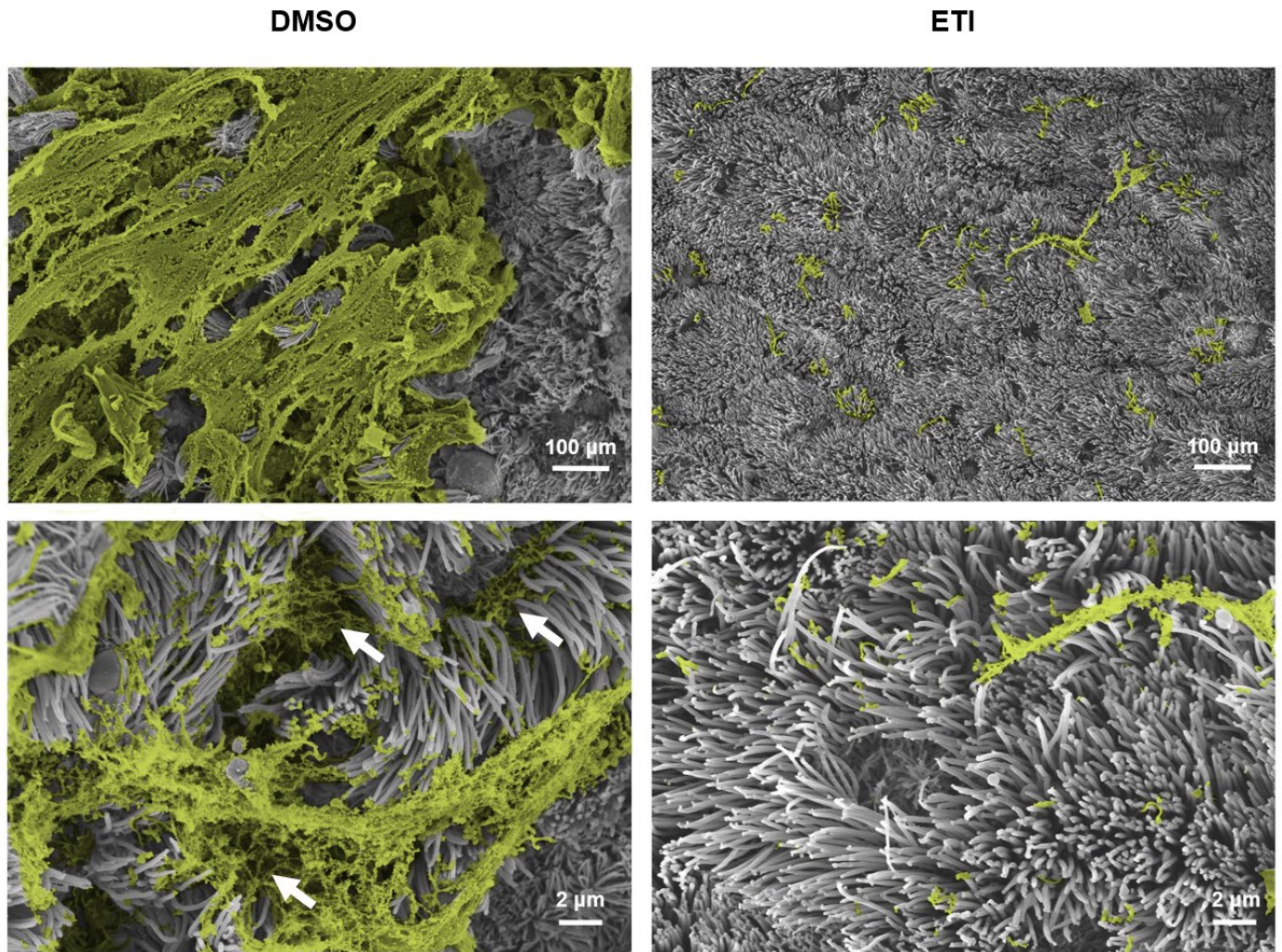


Figure S4. Colorized SEM micrographs shown in Figure 5. Representative SEM micrographs of DMSO- or ETI-treated F508del HBE cells showing an apical view of the inserts at low (top images) and high (bottom images) magnification power. To facilitate mucus discernment, the mucin network was colorized in yellow in the images. White arrows indicate the presence of mucus penetrating below the cilia tips.

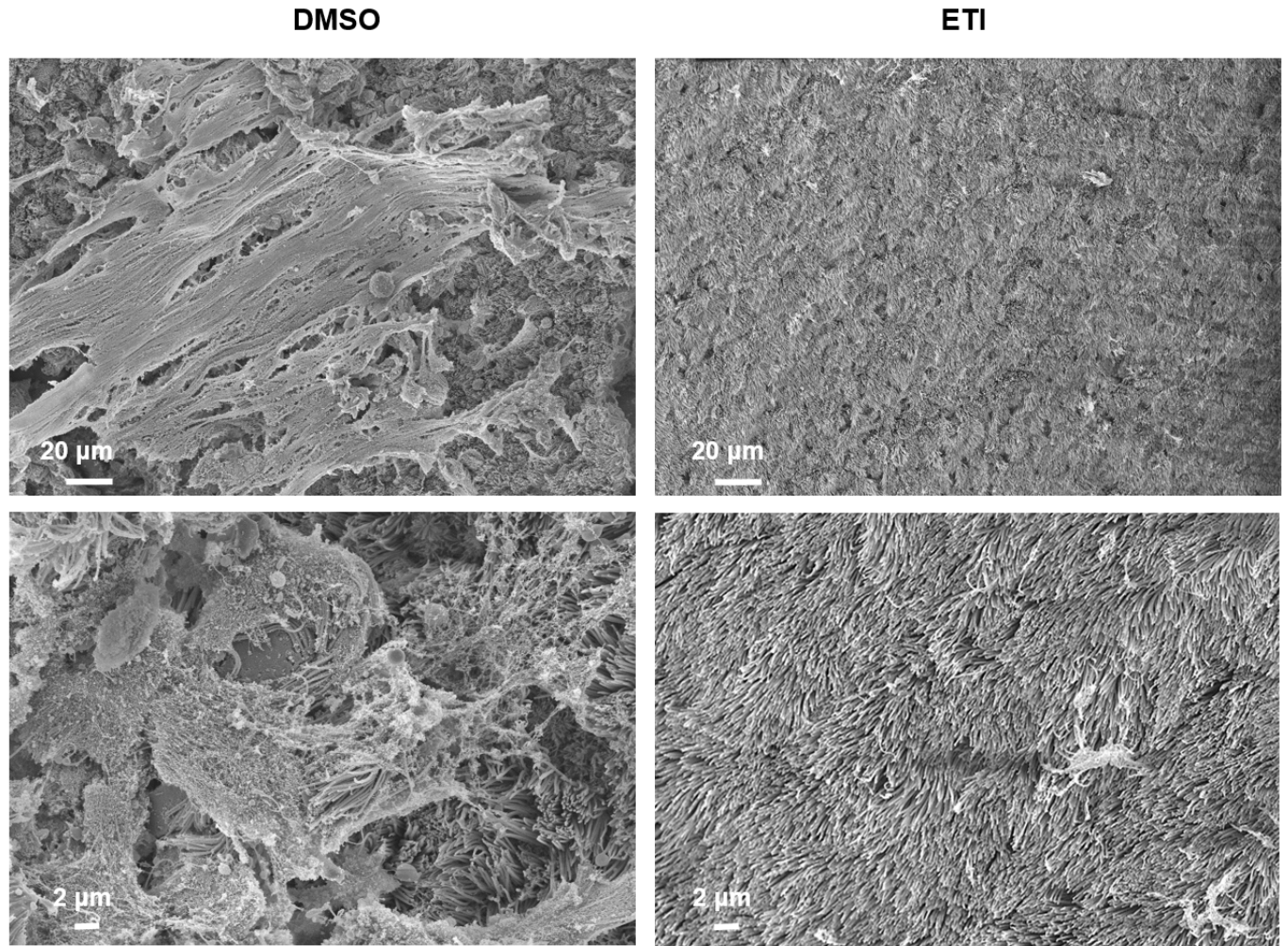


Figure S5. Additional inserts of F508del HBE cells treated with DMSO or ETI were imaged by SEM . Primary HBE cells homozygous for F508del were treated for 3 days with 0.06% DMSO or 3μM VX-661, 2μM VX-445 and 1μM VX-770 (ETI) before imaging. Micrographs show an apical view of the inserts at low (top images) and high (bottom images) magnification power.

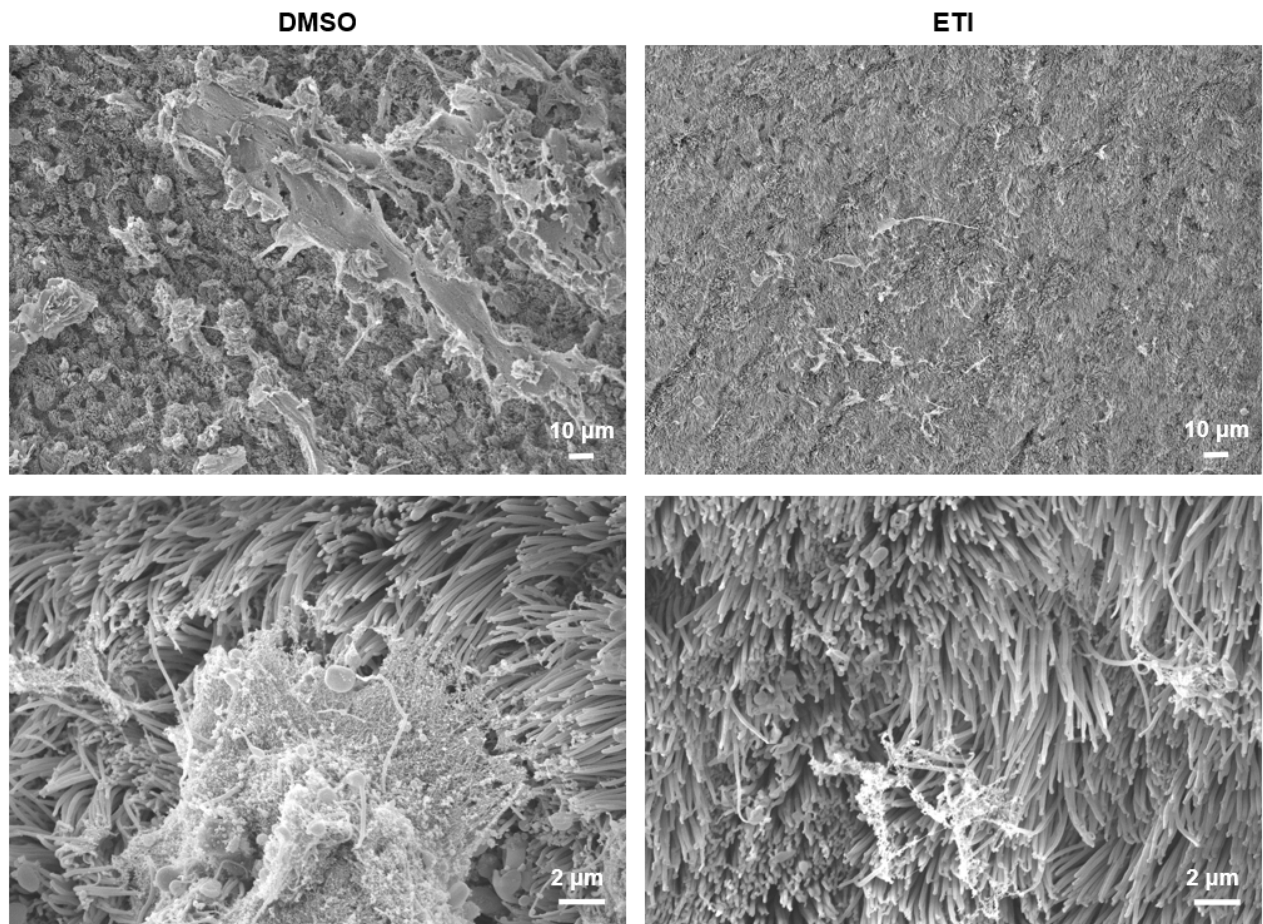


Figure S6. Additional inserts of F508del HBE cells treated with DMSO or ETI imaged by SEM. Primary HBE cells homozygous for F508del were treated for 3 days with 0.06% DMSO or 3μM VX-661, 2μM VX-445 and 1μM VX-770 (ETI) before imaging. Micrographs show an apical view of the inserts at low (top images) and high (bottom images) magnification power.

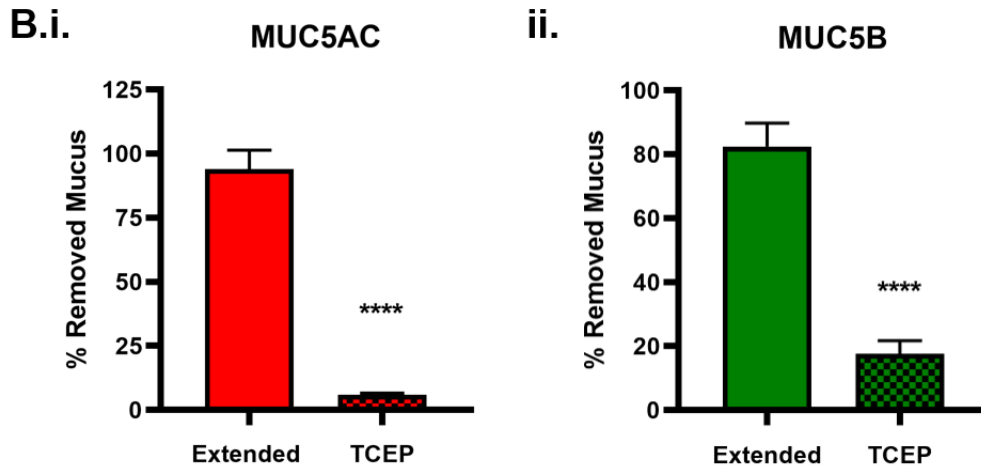
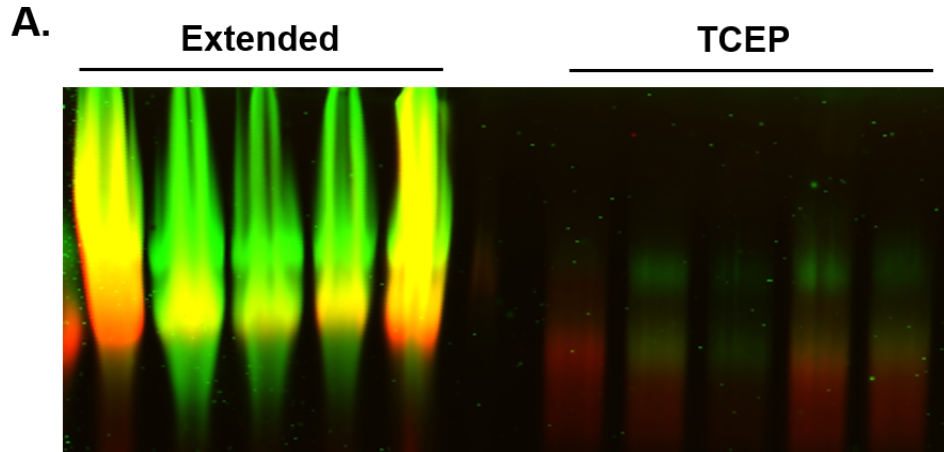


Figure S7. Extended wash removes the majority of apical mucus in CF HBE cell cultures.

A.) Western blot showing the MUC5AC (red) and MUC5B (green) signal of cell washings collected by 3h apical wash (extended), followed by an additional 15 min 1mM TCEP wash (TCEP). To normalize running conditions, 1 mM TCEP was added to the extended washes subsequently to collection. All samples were quenched after 15 min. **B.)** Graphs reveal the percent signal intensity of extended vs TCEP washes for MUC5AC (**i.**) and MUC5B (**ii.**). Extended washes removed 94% and 83% of total MUC5AC and MUC5B, respectively. **** $P < 0.0001$, Student's t-test. Error bars indicate SEM.

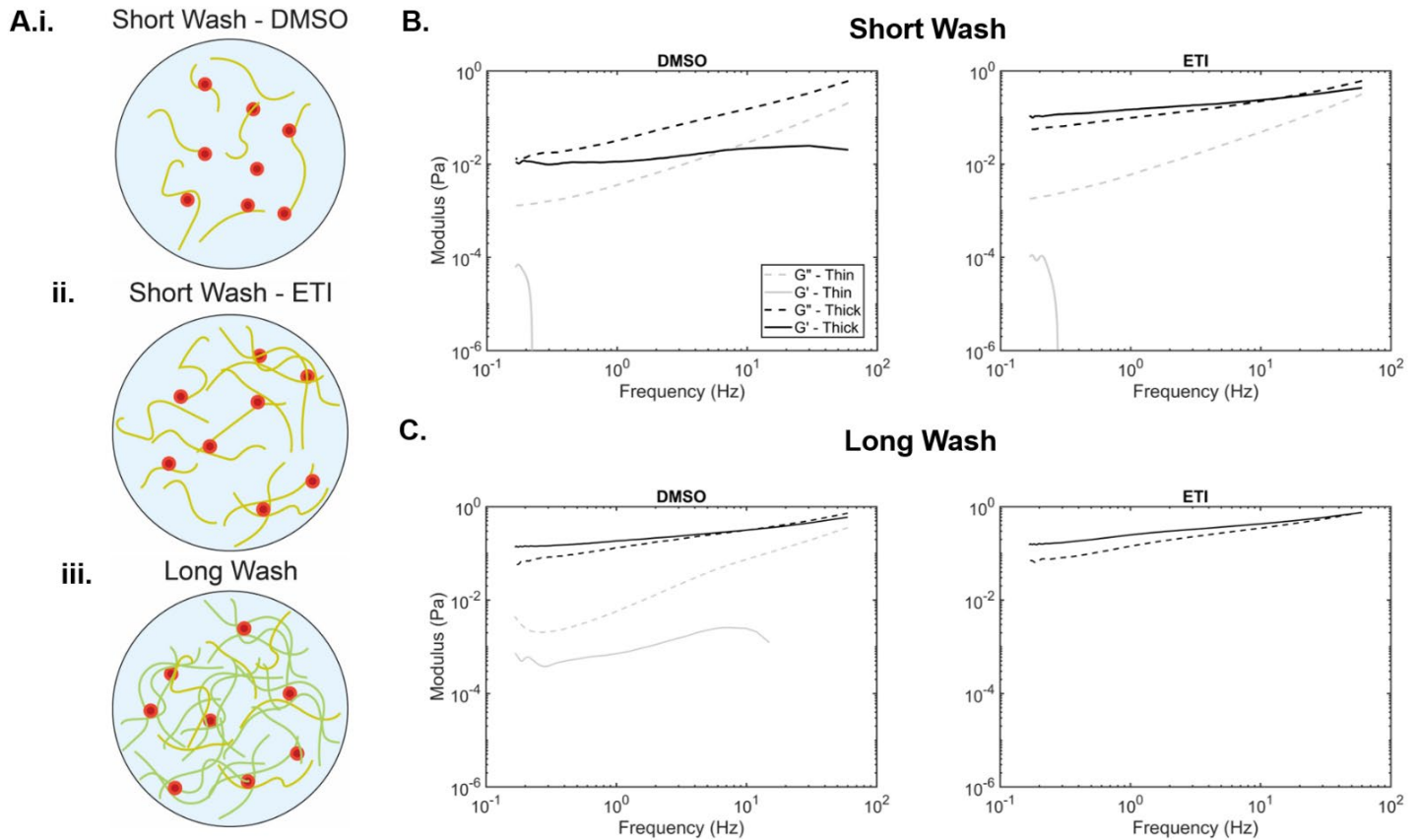


Figure S8. Elastic (G') and Viscous (G'') moduli of cell washings from Figure 8. A.) Depictions of the mucin polymer behavior in cell washings with added beads (red) (not to scale). Short washings from control cultures appeared as soluble, unentangled polymer solution (i.) and from ETI-treated cultures as a more concentrated polymer solution (ii.). Long washings are shown as a mixture of readily-soluble and slow-swelling mucins for both the vehicle- and ETI-treated cultures (iii.). **B.)** Elastic (G') and viscous (G'') moduli of cell washings from Figure 8 are shown as dashed and solid lines, respectively. Grey lines represent G' and G'' for beads/particles in the “thin” fraction, while black lines represent G' and G'' for beads/particles in the “thick” fraction at increasing frequencies. Note, sol/gel phase transition occurs when $G' \geq G''$ or when dashed a solid lines intersect. Short washes on DMSO-treated cells did not display a true gel-like behavior (i.e., neither grey nor black lines intersected), whereas ETI-treated cell washings exhibited a gel-like response in their thick cluster (i.e., black lines intersected). **C.)** Long washes on both DMSO- and ETI-treated cells yielded a thick, gel-like viscoelastic mucus.

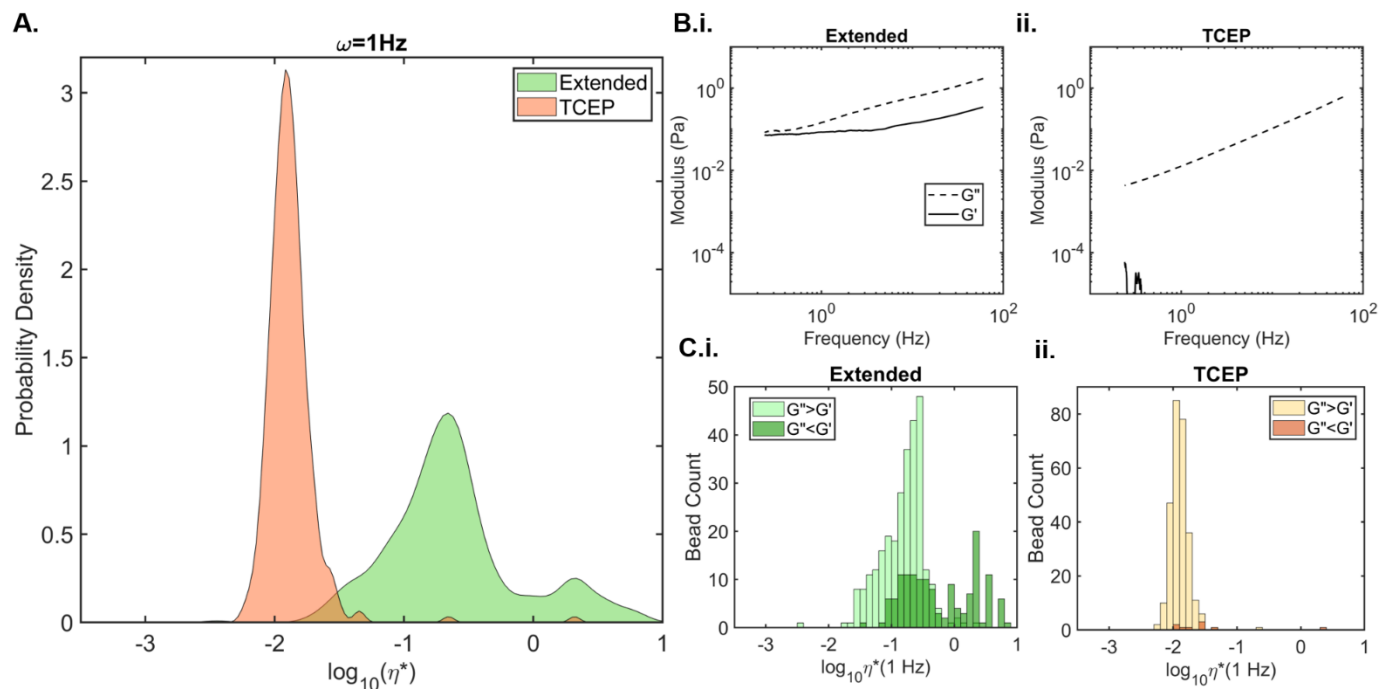


Figure S9. Viscoelastic properties of extended washes on naïve CF HBE cells with and without TCEP treatment. Naïve CF HBE cell cultures were washed for 3h with Krebs Ringer (extended) and analyzed by particle tracking microrheology (PTM). In parallel, extended washings were treated ex vitro with 1 mM TCEP (TCEP) for 15 min, quenched, and analyzed by PMT. **A.)** Histograms of complex viscosity (η^*) revealing bead probability density of extended (green) and TCEP (orange) washes. TCEP treatment resulted in a rheologically uniform solution (i.e., one narrow peak) with reduced viscosity compared to extended washes without TCEP treatment (i.e., two wide peaks). **B.)** Elastic (G' or solid line) and viscous (G'' or dotted line) moduli of extended (**i.**) and TCEP cell washings (**ii.**). Overall, mucus collected by extended washes behaved like a viscoelastic fluid, while mucus treated with TCEP behaved as a sol with no elastic response (i.e., considerably low frequencies). **C.)** Viscoelastic response of individual beads showing the average behavior of extended (**i.**) and TCEP-treated washes (**ii.**). Extended washes contained a mixture of beads that sensed a sol-like (light green) and a gel-like phase (dark green). TCEP-treated washes contained nearly all the beads in a sol phase (light orange) and hardly any beads in a gel-like phase (dark orange).

Videos 1-8: Representative videos of MCT velocity from Figure 5 of NT (videos 1-4) and ETI-treated (videos 5-8) primary F508del HBE cell cultures.

References

1. Hao S, Roesch EA, Perez A, Weiner RL, Henderson LC, Cummings L, Consiglio P, Pajka J, Eisenberg A, Yeh L, Cotton CU, Drumm ML. Inactivation of CFTR by CRISPR/Cas9 alters transcriptional regulation of inflammatory pathways and other networks. *J Cyst Fibros* 2020: 19(1): 34-39.
2. Ehre C, Worthington EN, Liesman RM, Grubb BR, Barbier D, O'Neal WK, Sallenave JM, Pickles RJ, Boucher RC. Overexpressing mouse model demonstrates the protective role of Muc5ac in the lungs. *Proc Natl Acad Sci U S A* 2012: 109(41): 16528-16533.
3. Fulcher ML, Gabriel S, Burns KA, Yankaskas JR, Randell SH. Well-differentiated human airway epithelial cell cultures. *Methods Mol Med* 2005: 107: 183-206.
4. Randell SH, Fulcher ML, O'Neal W, Olsen JC. Primary epithelial cell models for cystic fibrosis research. *Methods Mol Biol* 2011: 742: 285-310.
5. Gentzsch M, Cholon DM, Quinney NL, Boyles SE, Martino MEB, Ribeiro CMP. The cystic fibrosis airway milieu enhances rescue of F508del in a pre-clinical model. *Eur Respir J* 2018: 52(6).
6. Chen G, Ribeiro CMP, Sun L, Okuda K, Kato T, Gilmore RC, Martino MB, Dang H, Abzhanova A, Lin JM, Hull-Ryde EA, Volmer AS, Randell SH, Livraghi-Butrico A, Deng Y, Scherer PE, Stripp BR, O'Neal WK, Boucher RC. XBP1S Regulates MUC5B in a Promoter Variant-Dependent Pathway in IPF Airway Epithelia. *Am J Respir Crit Care Med* 2019.
7. Henderson AG, Ehre C, Button B, Abdullah LH, Cai LH, Leigh MW, DeMaria GC, Matsui H, Donaldson SH, Davis CW, Sheehan JK, Boucher RC, Kesimer M. Cystic fibrosis airway secretions exhibit mucin hyperconcentration and increased osmotic pressure. *J Clin Invest* 2014: 124(7): 3047-3060.
8. Ramsey KA, Rushton ZL, Ehre C. Mucin Agarose Gel Electrophoresis: Western Blotting for High-molecular-weight Glycoproteins. *J Vis Exp* 2016(112).
9. Markovetz MR, Subramani DB, Kissner WJ, Morrison CB, Garbarine IC, Ghio A, Ramsey KA, Arora H, Kumar P, Nix DB, Kumagai T, Krunkosky TM, Krause DC, Radicioni G, Alexis NE, Kesimer M, Tiemeyer M, Boucher RC, Ehre C, Hill DB. Endotracheal tube mucus as a source of airway mucus for rheological study. *Am J Physiol Lung Cell Mol Physiol* 2019: 317(4): L498-L509.
10. Carpenter J, Lynch SE, Cribb JA, Kylstra S, Hill DB, Superfine R. Buffer drains and mucus is transported upward in a tilted mucus clearance assay. *Am J Physiol Lung Cell Mol Physiol* 2018: 315(5): L910-L918.
11. Morrison CB, Markovetz MR, Ehre C. Mucus, mucins, and cystic fibrosis. *Pediatr Pulmonol* 2019: 54 Suppl 3: S84-S96.